International Journal of Microwave and Wireless Technologies, 2015, 7(3/4), 433–441.
doi:10.1017/S1759078715000690

RESEARCH PAPER

Target modeling and deduction of automotive radar resolution requirements for pedestrian classification

EUGEN SCHUBERT[1], MARTIN KUNERT[1], FRANK MEINL[1] AND WOLFGANG MENZEL[2]

Pedestrian Collision Mitigation Systems (PCMS) are already in the market for some years. Due to continuously evolving EuroNCAP regulations their presence will increase. Visual sensors, already capable of pedestrian classification, provide functional benefits, because the reaction behavior can be optimized when the imminent collision object is recognized as pedestrian or cyclist. Nevertheless their performance will suffer under adverse environmental conditions like darkness, fog, rain or backlight. Even in such unfavorable situations the performance of radar sensors is not significantly deteriorated. Enabling classification capability to automotive radar will further improve road safety and will lower PCMS's overall costs. In this paper, a multi-reflection-point pedestrian target model based on motion analysis is presented. Together with an appropriate sensor model, pedestrian radar signal responses can be provided for a wide range of accident scenarios. Additionally velocity separation requirements that are needed for classification of pedestrians are derived from the simulations. Besides determination of classification features, the model discloses the limits of classical radar signal processing and further offers the opportunity to evaluate parametric spectral analysis. Based on simulated and measured baseband radar signals of pedestrians one of these techniques is deeper analyzed and its enhancement especially on the velocity separation capability is evaluated.

Keywords: Radar applications, Radar signal processing and system modeling

Received 13 October 2014; Revised 19 March 2015; Accepted 22 March 2015; first published online 16 April 2015

I. INTRODUCTION

According to the Euro NCAP Roadmap Pedestrian Collision Mitigation Systems (PCMS) will be rated as from 2016. Although modern PCMS are able to handle these tests, improving the performance will still go on. After 2016 next generation PCMS are expected to not just activate the brakes of a car. Algorithms based on adaptive parameterized pedestrian tracking will be used to determine the most suitable emergency manoeuvre out of a diversity of possible mitigation strategies. Thereby, highest collision mitigation is achieved while simultaneously preventing unjustified system interventions [1]. To adapt target tracking algorithms to several object classes, like pedestrians, reliable classification algorithms are necessary. Because of its advantages compared with other sensing technologies, radar will be one of the essential sensor technologies in future PCMS. However, one deficiency of modern automotive radar sensors is still the lack of reliability in pedestrian classification. Addressing this functionality within future generations of radar sensors will increase road safety especially under adverse weather conditions, like fog, rain or visual reflections of headlights on wet roads. The value of already existing safety functions will be increased by reliable classification of critical objects like pedestrians because of a higher level of driver's acceptance of automatic interventions in situations pedestrians are involved. Additionally unjustified system responses will be suppressed. For instance, the activation of an active bonnet only in case of an expected, well-classified pedestrian impact will minimize maintenance effort and associated costs. First approaches in automotive radar-based pedestrian classification mostly rely on the evaluation of object's range and velocity spreads [2].

In this paper, a multipoint radar target model capable of simulating high resolution radar responses of most relevant pedestrian accident scenarios is presented. Detailed results of a well suited approach of motion analysis are discussed, followed by the description of development and integration of the target model in an automotive radar simulation environment. Finally, simulation results of pedestrian accident scenarios and deduced features for pedestrian classification are presented. Additionally the impact of applying autoregressive spectral signal analysis to resolution and classification features is evaluated both with simulations and measurements.

[1]Robert Bosch GmbH, Chassis Systems Control, Advanced Engineering Sensor Systems, P.O. Box 16 61, 71226 Leonberg, Germany
[2]Ulm University, Institute of Microwave Techniques, Ulm, Germany
Corresponding author:
E. Schubert
Email: eugen.schubert@de.bosch.com

II. HUMAN MOTION ANALYSIS

Based on observations of pedestrians with a 24 GHz Pulse-Doppler radar, a six point model representing feet, knees, and two points of the upper body is developed in [3].

Thereby the movements of the legs are approximated by sinusoidal oscillations in the direction of motion superimposed to the motion of the center of gravity (CoG). Swinging arms are neglected. A more detailed approach for pedestrian modeling to estimate human walking parameters is presented in [4]. Parameters, such as cycle frequency, cycle length or cycle phase are estimated and visualized with a human walking scene in virtual reality. In [5], high resolution 12.5 GHz inverse synthetic aperture radar (ISAR) is used for Doppler measurements of pedestrians. Human motion simulation and measurements are compared to define the constraints of image processing radar. Thereby two-dimensional radar images were simulated from motion data partially obtained from [6] with respect to seven distinctive points (sternum, hands, knees, and toes). However, simulations of pedestrian accident scenarios are very rarely addressed in literature. Most existing target models underlay simplifications which could affect the derivation of classification features. Further on, observations of pedestrians in literature are often based on measurement principles, like synthetic aperture radar (SAR) or ultra wideband radar (UWB), that do not suitably match automotive requirements in terms of sensor size or available bandwidth.

In this work, a simple but well suited measurement setup is used to develop a pedestrian target model. Motion sequences of test persons, tagged at the feet (FR/FL), knees (KR/KL), hands (HR/HL), elbows (ER/EL), right shoulder, right hip, and head (H), were recorded cinematically with a frame rate of up to 240 fps to obtain the space-time information of different body parts. Velocity-time functions have been derived through numerical differentiation and low pass filtering. Figure 1(a) displays the measured space versus time functions and Fig. 1(b) the speed versus time functions of each body part. Because of the linear uniform movement of the head, its function is considered to be representative for the pedestrian's CoG. Closer look at the speed-time-functions shows that they do not follow an ideal sinusoidal shape, as simple models in literature propose [3]. This must be kept in mind when pedestrians shall be realistically represented during system assessment by articulating dummies, capable of arm and leg movement. Different lengths of arms and legs result in different velocity amplitudes. Furthermore it is obvious from the records that the body parts are accelerated several times during one gait cycle. Thereby the feet reach the highest spread in the velocity domain of approximately three times the mean value. Caused by the rolling motion of

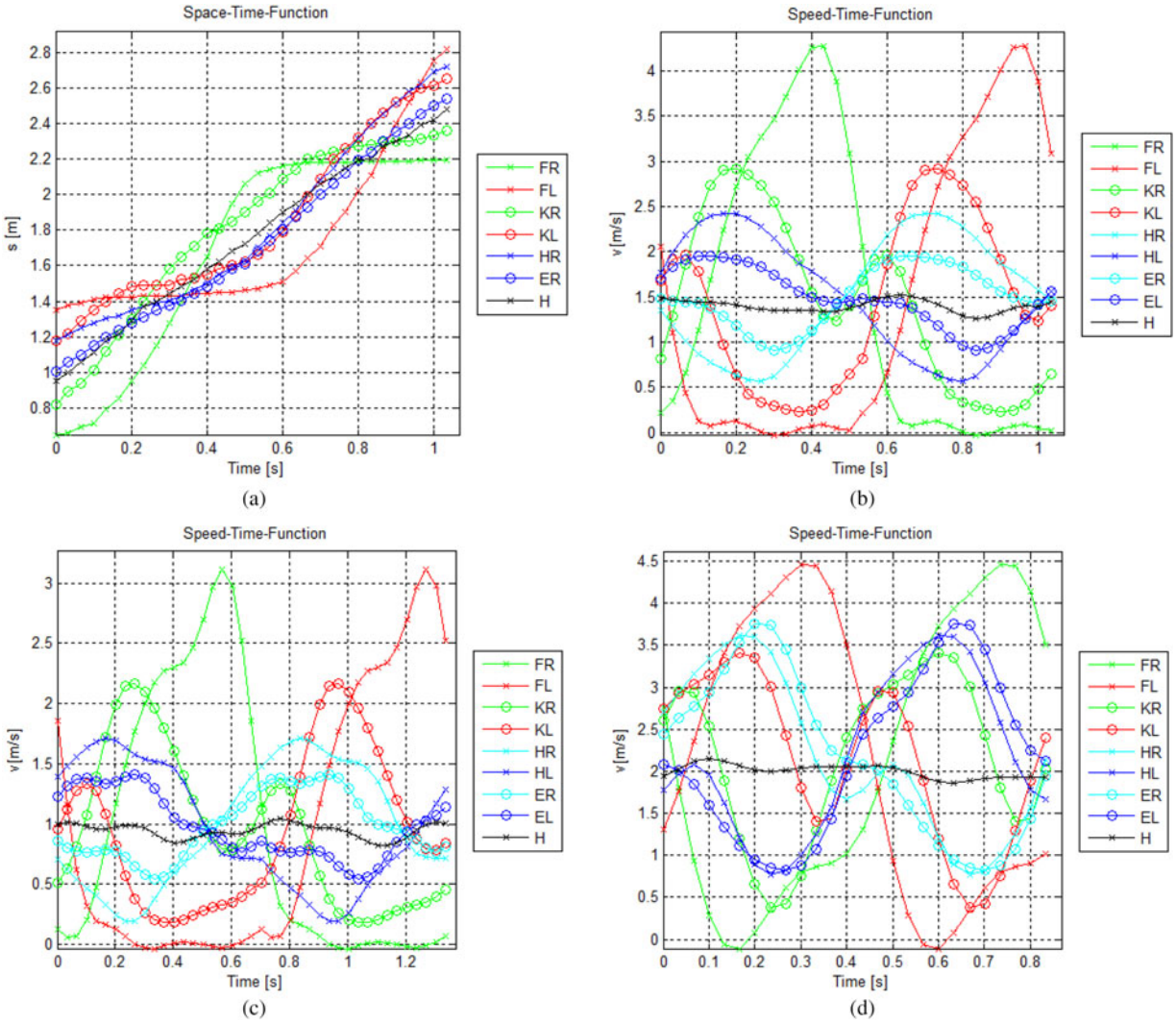

Fig. 1. Space-Time-Function of a walking pedestrian (a) and Speed-Time-Functions of a walking (b), strolling, (c) and jogging (d) pedestrian (FR/FL: foot right/left, KR/KL: knee right/left, HR/HL: hand right/left, ER/EL: elbow right/left, H: head).

https://doi.org/10.1017/S1759078715000690 Published online by Cambridge University Press

Table 1. Characteristic values of different paces.

	Strolling	Walking	Jogging
v_{mean} [m/s]	0.95	1.43	2.20
v_{max} [m/s]	3.08	4.30	4.60
f_{step} [Hz]	0.75	0.97	1.20
s_{step} [m]	1.28	1.47	1.75

the feet, their velocities reach zero only for a distinct amount of time while other body parts are in motion over the whole gait cycle. Caused by the cinematic measurement method the positions of the left body parts could not be measured continuously. Nevertheless the measured data are sufficient enough to prove the assumption that the motion patterns of left and right extremities are identical with exception of a phase shift of pi, as can be seen in the space time functions given in Fig. 1(a).

For further investigations on the influence of the walking speed to the maximum velocity, step frequency and step length measurements of different paces of a person were conducted. Figures 1(c) and 1(d) show the speed time functions of strolling and jogging motion. Characteristic values of the different speed-time-functions are listed in Table 1. Thereby the step frequencies and step lengths are given in relation to the motion of single legs. Given the minor difference between the peak velocity during walking and jogging, the existence of an upper border for the peak velocity can be assumed. For faster paces the increased mean value is achieved rather by a broader shape of the curve than by the increase of the peak velocity. Furthermore, in case of faster movement, sinusoidal approximation of the velocity functions is nearly justifiable. The results gained with the presented approach are quite comparable with the findings of more sophisticated measurement methods of [5, 6] and therefore highly suitable for simulation model development.

III. SIMULATION ENVIRONMENT

A) Sensor model

A sensor model featuring chirp sequence modulation provides the advantage of unambiguous range and velocity determination. Thereby K frequency modulated continuous wave signals are consecutively transmitted. The reflected and down converted signal of a single reflecting point with radial velocity v_r and radial distance d_r is described by

$$s_{IF}(t) = e^{2\pi j\left(\left[2f_c \cdot d_r\right]/c_0\right)} \cdot \sum_{k=0}^{K-1} e^{2\pi j\left[\left\{\left(2f_c \cdot v_r \cdot T_{RRI} \cdot k\right)/c_0\right\} + \left(\left\{\left(2f_c \cdot v_r\right)/c_0\right\} + \left\{\left(2B \cdot d_r\right)/T \cdot c_0\right\}\right) \cdot t\right]} \cdot rect\left(\frac{t - k \cdot T_{RRI}}{T}\right), \quad (1)$$

with single-chirp duration T, bandwidth B, carrier frequency f_c, chirp repetition interval T_{RRI}, and the chirp number k of a chirp sequence of length $K-1$ [7]. Consequently, the radar target model of the pedestrian must provide the radial range and velocity of all considered reflection points for each time step of a given scenario. Characteristic values of the used modulation are given in Table 2. These values ensure results with high resolution and excellent target separability. With regards to state of the art update rates of automotive radar sensors a dead time was implemented between the chirp sequences for taking into account the processing time of the sensor. Of course the maximum detection range of 76 m is not suitable for all automotive radar applications but it is considered as sufficient for pedestrian detection at vehicle velocities of up to 100 km/h.

Table 2. Modulation characteristics.

Parameter	Value	Parameter	Value
f_c	76.5 GHz	Cycle rate	20 Hz
B	1 GHz	Δv_r (resolution)	0.15 m/s
T	20 µs	Δd_r (resolution)	0.15 m
TRRI	25 µs	$d_{r,max}$	76 m
K	512	$v_{r,max}$	39 m/s

B) Pedestrian target model

To determine analytical velocity versus time and space versus time functions of each reflection point of the pedestrian target model, the measured data of Fig. 1 were processed by a Fast Fourier Transform (FFT). Each velocity function can be represented by the sum of a small amount of oscillations depending on a set of complex Fourier coefficients c_k.

$$v(t) = \frac{c_{mean}}{c_0} \cdot \sum_{k=-\infty}^{\infty} c_k e^{j2\pi k f_0 t}. \quad (2)$$

Thereby f_o denotes the sample frequency of the camera which was used for the cinematic measurements described in Section II. To compensate slight measurement uncertainties the steady components are rescaled to a common mean value c_{mean}, corresponding to v_{mean} of Table 1. Integration of (2) results in space-time representation

$$s(t) = c_{mean} \cdot t + \sum_{k=-\infty}^{\infty} \frac{c_{mean}}{c_0} \frac{c_k}{j2\pi k f_0} \left(e^{j2\pi k f_0 t} - 1\right) + s_0, \quad k \in Z^*, \quad (3)$$

of the different body parts. Thereby the integration constant was replaced by the position offsets (s_0) between the CoG and each body part at the beginning of the gait cycle. Given (2) and (3) and the parameter set of c_k enables the simulation of a multiple point pedestrian motion model for any desired time length. In the last step the functions were transformed into a radial coordinate system of the sensor model and included in the Matlab-based simulation environment. By providing adjustable parameters such as starting point, direction angle, vehicle velocity, and simulation duration, this environment enables the simulation of radar signal responses of most relevant accident scenarios without the need to run dangerous or life-threatening real-world tests.

To provide realistic radar signal responses the different reflection points of the human body feature different Radar cross-sections (RCS). The signal levels are approximated by simply combining the mean RCS value of a pedestrian in the 76 GHz band that is −6.6 dBsm [8] with the partial distribution of the body surfaces according to [9]. The RCS used for the different body parts are listed in Table 3. Additionally a factor to model the free space loss was implemented.

https://doi.org/10.1017/S1759078715000690 Published online by Cambridge University Press

Table 3. RCS values for simulation of reflection points.

Reflection-point	FR/FL	KR/KL	HR/HL	ER/EL	CoG
RCS [dBsm]	−20.7	−14.2	−23.6	−18.6	−10.4

Measurements with a radar sensor in the 76 GHz band were performed in an anechoic chamber to verify the developed model. Thereby the same modulation parameters, as provided in Table 2, were used. Figure 2 shows the simulated (a) and measured (b) Range-Doppler (RD) response of a radial walking pedestrian developed over one 10 ms long chirp sequence recorded at the point in gait cycle at which the speed of 1 ft reached its maximum of approximately 4 m/s (e.g. at time instant of 0.35 s in Fig. 1(b)). Besides ground clutter presence and minor RCS differences, both RD responses show very similar distributions of velocities. The nine points used for simulation are just enough to sufficiently approximate the main reflection points of a pedestrian's radar signal response. Especially the velocity spread, which is needed to develop and test classification algorithms, is comparable. However, to generate an accurate radar backscatter signal of a pedestrian with a high level of detail the use of a model with more reflection points or even a simulated body with continuous surface, comparable with real pedestrians, is recommended.

IV. ACCIDENT SCENARIO SIMULATION

A closer look on the distribution of accident scenarios shows, that pedestrian accidents in real world happen not exclusively in scenarios proposed by Euro NCAP tests [10]. A real world interpretation of an exemplarily taken test of the NCAP protocol is illustrated in Fig. 3(a). Furthermore, a significant amount of accidents with killed or seriously injured pedestrians occurs in additional scenarios like: "Along the carriageway on a straight road without obstruction" (Fig. 3(b)). A system capable to indicate the presence of pedestrians under adverse visibility conditions, like rain, fog or darkness in combination with wet roads and related reflecting backlight, may be a good opportunity for radar-based pedestrian classification to enter the market.

An automatic triggered pedestrian warning enables the driver to adapt his driving behavior faster and consequently helps to avoid potential safety-critical situations. For PCMS capable of automatic interventions the classification algorithms increase system robustness and decrease the false intervention rate.

In state of the art automotive radar signal processing, where high resolution leads also to a high amount of backscattering points, several detected reflections are clustered to a lower amount of hypothesized objects. State variables, such as position, speed or additional properties of these objects are then further processed by appropriate tracking algorithms like a Kalman-Filter. Additionally such a formed group of reflections can also be used for classification of the objects by analyzing the expansion in speed or range inside the cluster. Classification results will be more reliable if more reflections per object can be separated by the radar. To separate reflections three domains are available for radar signal processing: range, velocity or angular domain. The minimum requirement for separation of at least two reflections of the same domain scattered by one real object is that the radar's resolution cell is smaller than half of the objects expansion in the specific domain. To determine separability requirements for pedestrian classification in range, velocity, and angle, pedestrian expansions were analyzed by simulation of

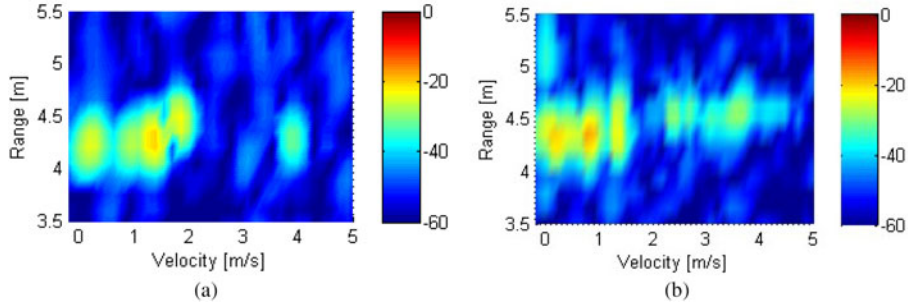

Fig. 2. Simulated (a) and measured (b) RD response of a walking pedestrian.

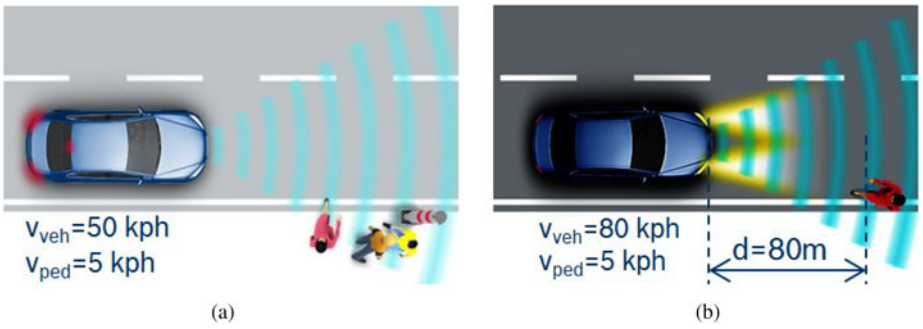

Fig. 3. Accident scenarios: (a) crossing pedestrian in a simplified urban area and (b) along a carriageway during darkness.

https://doi.org/10.1017/S1759078715000690 Published online by Cambridge University Press

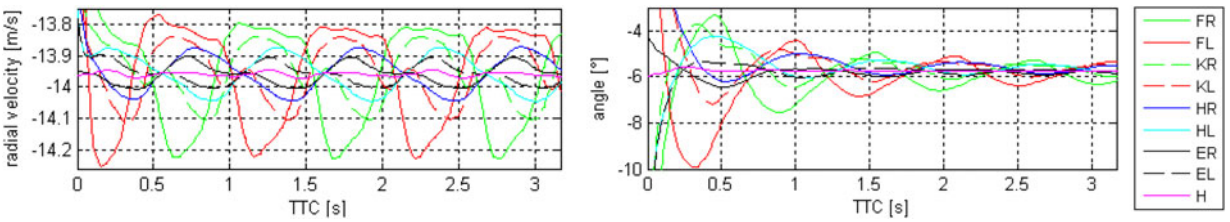

Fig. 4. Trajectories of radial velocities and angles of different body parts versus TTC of a crossing pedestrian scenario with the aim to obtain the necessary separation requirements.

the trajectories of pedestrian body parts in different significant accident scenarios. Figure 4 exemplarily illustrates the curves of the velocities and angles over time to collision (TTC) of the simplified urban crossing scenario introduced in Fig. 3(a).

The expansion in velocity domain can be obtained to a range of 0.15–0.45 m/s and the expansion in angular domain to less than 0.5° at 3 s and to ca. 2.5° at 1 s before impact. Based on human geometry the minimum expansion in range is simply approximated to 0.5 m. Given those values and a closer consideration of limitations in bandwidth and sensor size, the conclusion that the velocity domain seems to be the most suitable to determine separation requirements can be drawn, which are achievable by state of the art and near future radar systems.

For demonstration of the classification potential of high resolution radar, Fig. 5 provides simulated RD responses cumulated over several successive chirp sequences for different scenarios. A comparison between Figs 5(a) and 5(b) shows the principle possibility to discriminate a longitudinal walking pedestrian from a static target next to the road by evaluating the velocity distribution – even several seconds before a possible collision may occur. Nevertheless the velocity spread should not be the one and only feature for robust classification algorithms. A lot of additional effects are present in real urban scenarios like the presence of multiple pedestrians within the same resolution cell or multipath and interference issues. These effects could lead to velocity spreads similar to those of pedestrians. To overcome these issues high resolution radar enables to distinguish between several scattering points of one physical object. Additional features like the estimation of multidimensional object size or further statistical analysis should be derived after grouping of detections to develop robust pedestrian classification with low false alarm rate.

Especially scenarios with lateral moving pedestrians and high vehicle velocities, as illustrated in Fig. 3(a), are challenging for radar-based pedestrian classification, because of smaller angles and corresponding smaller contributions to the radial velocities. Figure 5(c) shows the RD responses cumulated over time of such a scenario. Even if some differences can be recognized by comparing the shapes of Figs 5(a) and 5(c), a clear separation of different reflection points by their velocities is not reliably possible. Nevertheless a wide spread of the detected velocities around their mean values can be still observed over time. This is caused by the different RCS of the body parts and the fact that radar backscatter always responds the superposition of non-resolvable reflection points. Evaluation of the velocity's variance over time is also appropriate for classification of pedestrians in case of poor separability. This effect can also be seen in the distribution of the blue dots of Fig. 8.

V. INCREASING VELOCITY RESOLUTION BY SIGNAL EXTRAPOLATION

Improvement of the velocity separation capability of a microwave radar requires in general extending the measurement time and consequently decreasing the cycle rate of the sensor. Linear prediction based signal extrapolation may

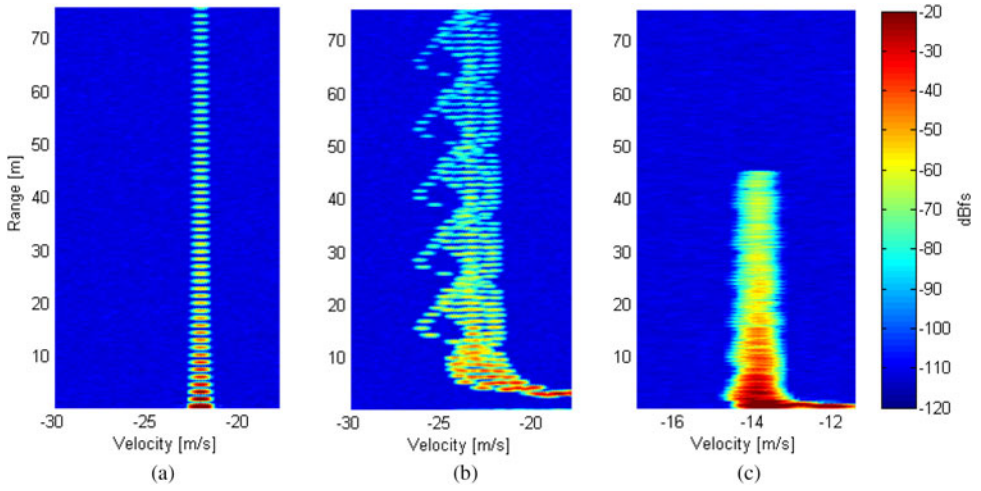

Fig. 5. RD responses of several measurement cycles cumulated over time for different scenarios: (a) approaching stationary target with 80 km/h and initial distance of 76 m; (b) approaching longitudinally walking pedestrian with 80 km/h and initial distance of 76 m; (c) approaching crossing pedestrian on collision course with $v_{veh} = 50$ km/h.

https://doi.org/10.1017/S1759078715000690 Published online by Cambridge University Press

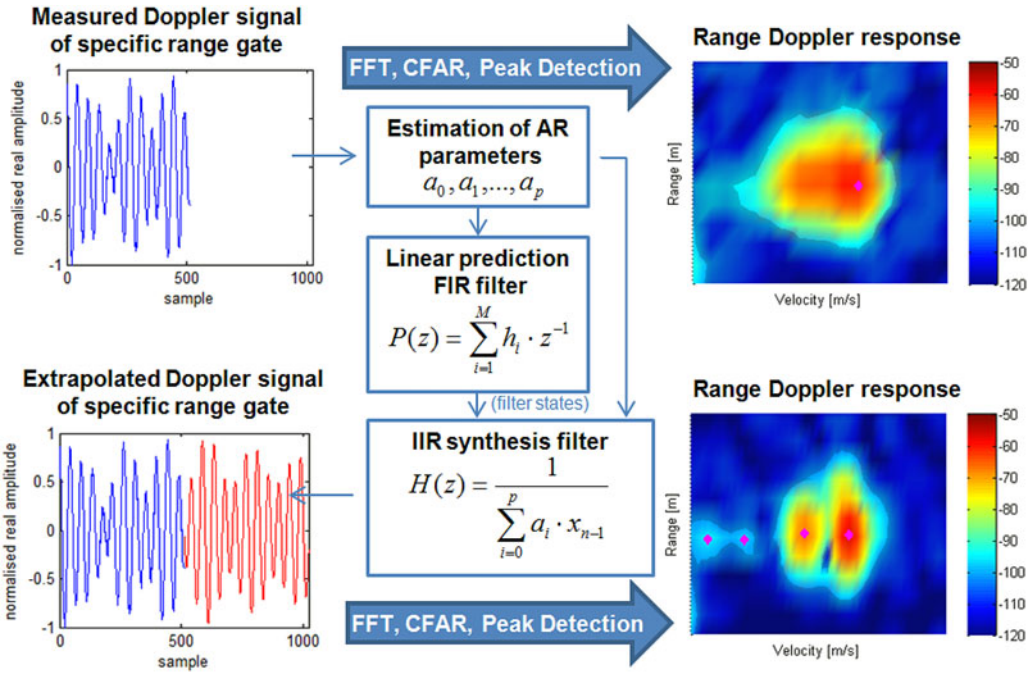

Fig. 6. Overview of the algorithm used for extrapolation applied to real measured data of a radial walking pedestrian.

offer solutions for this dilemma to some extent. The algorithm used for this section was adapted from [11] and its application to real measured data of a radial walking pedestrian is additionally illustrated in Fig. 6. With Linear Prediction theory previously unknown samples of a signal are generated from a few known samples by the use of the following equation and the corresponding linear prediction finite impulse response (FIR) filter

$$x_n = \sum_{i=1}^{M} h_i \cdot x_{n-1}, \quad P(z) = \sum_{i=1}^{M} h_i \cdot z^{-1}, \tag{4}$$

where x_n is the new sample predicted from the previous samples x_{n-1} and the prediction filter coefficients h_i [11].

The step-by-step application of (4) allows the prediction of an unlimited amount of new samples. In the straightforward approach h_i are determined by application of (4) to a known section of the signal and the minimization of the prediction error. Because the exact analytical solution only exists for noiseless theoretical signals for real radar signals another approach should be used [11]. The coefficients can be determined by autoregressive modeling algorithms like the Burg algorithm and relation

$$h = [h_1, \ldots, h_M] = [-a_1, \ldots, -a_p], \tag{5}$$

where $[a_o, \ldots, a_p]$, $a_o = 1$ are the $p + 1$ coefficients of an autoregressive model of the order p determined from the original signal. The step by step application of (4) can also be implemented with the infinite impulse response (IIR) synthesis filter

$$H(z) = \frac{1}{1 - P(z)} = \frac{1}{1 - \sum_{i=1}^{M} h_i \cdot x_{n-1}} = \frac{1}{\sum_{i=0}^{p} a_i \cdot x_{n-1}}, \tag{6}$$

fed with zero input vector of the length of the amount of samples to be predicted [11]. The needed initial conditions for this filter are either obtained by feeding the linear prediction FIR filter (4) with all samples of the original signal or by assuming the prediction of the last $p-1$ originally known samples by the IIR extrapolation filter.

As displayed in Fig. 6 the presented extrapolation algorithm can be applied to the Doppler signal which, according to chirp sequence signal processing, is formed by the complex spectral peaks of a specific range cell of successive chirps. A frequency analysis of this signal gives the spectrum of velocities for each range. Additional processing of Constant False Alarm Rate (CFAR) based noise threshold estimation and peak detection further leads to detected range velocity pairs, indicated by pink rhombuses in Fig. 6. Extrapolation increases the separability, which, for constant sample rate, directly depends on the number of samples. The resulting separability of the presented two-staged algorithm consisting of linear prediction based signal extrapolation and subsequent FFT spectral analysis could maximally be as good as the worst of each stage. In best case the separability of the FFT can be expected to be the double of the frequency resolution, whereas the separability of the AR spectra nonlinearly depends on signal power (SNR) and model order [12]. Figure 7 compares the separation capabilities of autoregressive spectral analysis with the classical Fourier spectrum separability, without application of a window to the time signal.

For proper increase of separability the AR model order should be chosen between the intersections of the dashed lines, illustrating the separability of the FFT for length of the original and extrapolated signal, with the lines of the SNR dependent separability of the AR spectral analysis. For highest possible separability enhancement the model order should be chosen according to the intersection with the red dashed line, e.g. for targets with 20 dB SNR an AR model order of 60 would be appropriate in case 512 original samples should be extrapolated to 1024 samples.

https://doi.org/10.1017/S1759078715000690 Published online by Cambridge University Press

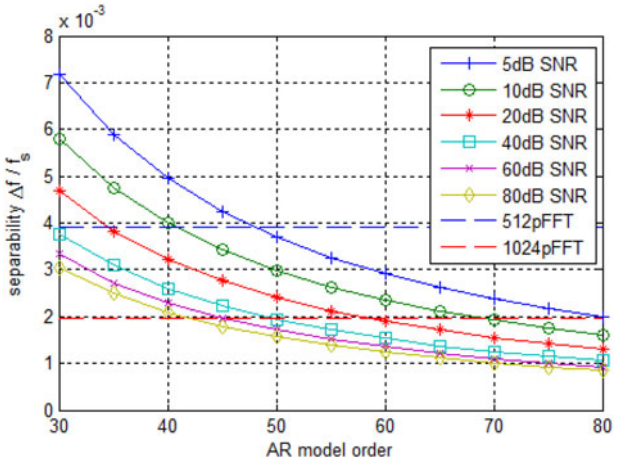

Fig. 7. SNR and model order dependency of AR model spectral separability in comparision with seperability of FFTs with 512 or 1024 points and no windowing applied.

To validate the obtained gain in resolution and separability, Fig. 8 shows the detections over time (blue dots) determined by classical radar signal processing of 512 samples long simulated signals in comparison with the detections determined by processing simulated signals extrapolated to 1024 samples (red rhombuses) of the lateral walking scenario presented in Fig. 3(a). Doubling the number of samples increases the spectral velocity separation from 0.3 to 0.15 m/s and enables separation especially of the legs and feet from the body, at least during the times of gait cycle when the feet reaches maximum velocity. A further comparison of the detections with the velocity functions of the underlying pedestrian motion model shows that the additional detections determined by an analysis of the extrapolated signal are mainly based on the pedestrian's model functions than on random effects or noise. To prevent possible disturbing influence the same CFAR algorithm was used for both analyses.

The improved separation capability compared with classical radar detection algorithms increases the number of detectable range Doppler pairs within one physical object. Adequate grouping of these pairs to hypothesized objects enables estimation of additional features for object classification.

For additional validation the algorithm was applied to real data measured from a radial walking pedestrian. The processed RD responses of the original and extrapolated baseband signals of 50 consecutive measurement cycles cumulated over time are given in Fig. 9. Thereby in sum about 400 reflections have been detected from the original signal whereas more than 500 could be detected after extrapolation. Additionally the narrower peaks and the corresponding increased separability in the spectrogram of the extrapolated signal can be seen in the circled areas. The peak widths especially in the velocity domain in the spectrum of the extrapolated signal are smaller compared with the spectrum of the original signal. This is caused by the application of signal windowing and

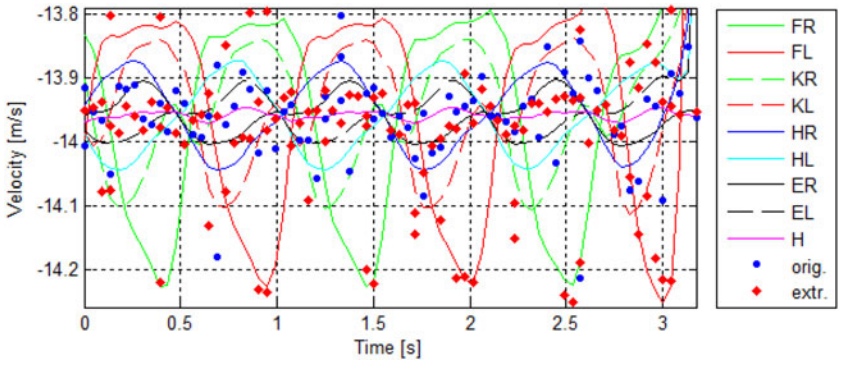

Fig. 8. Detections based on simulated signal (blue dots) and based on the extended simulated signal (red rhombuses) versus time of the crossing pedestrian scenario in comparison with the model based velocity functions.

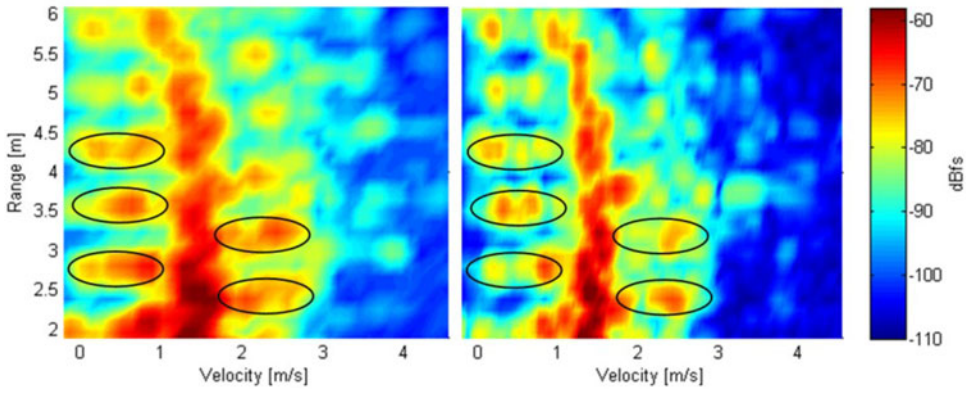

Fig. 9. RD responses of a radial walking pedestrian cumulated over 50 consecutive chirp sequences without signal extrapolation (left) and with application of extrapolation (right).

https://doi.org/10.1017/S1759078715000690 Published online by Cambridge University Press

FFTs of larger sizes with respect to the processing of the original signal.

In theory all relevant high resolution target information of the signal have already been included in the AR parameters or in the initial conditions and filter coefficients of the synthesis filter, respectively. A method to obtain signal parameters directly from the AR parameters is expected to achieve an even better separability because no separability deteriorating windowing function needs to be applied in contrast to Fourier analysis. For example, the frequencies of the original signal can be obtained directly from the roots of the characteristic polynomial of the FIR prediction filter. Unfortunately thereby the phase and amplitude information are lost in the first place and need to be recovered additionally. An advantage of the proposed method is that, besides enlargement, the classical radar signal processing chain consisting of FFT, CFAR, and peak picking algorithm can be maintained. Furthermore, the challenge of sensitive estimation of the ideal order of the autoregressive model is avoided because the proposed method seems to be more robust than the direct method against common known effects like spurious spectral peaks and line splitting caused by over fitting the model order. Another observed advantage is the fact that the synthesis filter only extrapolates predictable signal components. Because noise is not predictable doubling the samples halves the noise power in the spectrum of the extrapolated signal. This can also directly be recognized from the color of the noise levels of the spectrograms of Fig. 9. This effect supports especially the detection of smaller targets, whose amplitudes without extrapolation would be close beneath the CFAR threshold.

VI. CONCLUSION

Starting with a detailed pedestrian motion analysis a multi-reflection-point target model was developed to simulate radar reflection characteristics of a pedestrian in most relevant accident scenarios. Based on these, radar resolution and target separation requirements for pedestrian classification were derived. Additionally, the captured motion data provided in this paper can be further used to specify articulating dummies for system testing.

Because velocity resolution is proportional to measurement time, which is limited by cycle rate requirements, the potential of linear prediction based signal extrapolation increasing the separability in the velocity domain was investigated. Thereby the extrapolation algorithm was presented in detail and auspicious results based on simulated and measured baseband radar signals have been achieved.

REFERENCES

[1] Bräuchle, C.; Flehmig, F.; Rosenstiel, W.; Kropf, T.: Maneuver decision for active pedestrian protection under uncertainty, in IEEE Annual Conf. on Intelligent Transportation Systems, Netherlands, 2013, 646–651.

[2] Rohling, H.; Heuel, S.; Ritter, H.: Pedestrian detection procedure integrated into an 24 GHz automotive radar, in IEEE Int. Radar Conf., Washington DC, USA, May 2010, 1229–1232.

[3] Fölster, F.; Rohling, H.; Ritter, H.: Observation of a walking pedestrian with a 24 GHz automotive radar sensor, in German Microwave Conf., Karlsruhe, Germany, 2006.

[4] Dorp, P.v.; Groen, F.C.A.: Human walking estimation with radar. IEE Proc. Radar, Sonar Navig., **150** (5) (2003), 356–365.

[5] Ghaleb, A.; Vignaud, L.; Nicolas, J.M.: Micro-Doppler analysis of wheels and pedestrians in ISAR imaging. IET Signal Process., **2** (3) (2008), 301–311.

[6] Motion Capture Database of Carnegie Mellon University Graphics Lab, Pittsburgh, PA 15213, http://mocap.cs.cmu.edu

[7] Andres, M.; Menzel, W.; Bloecher, H.-L.; Dickmann, J.: Detection of slow moving targets using automotive radar sensors, in German Microwave Conf., Ilmenau, Germany, 2012, 1–4.

[8] Schubert, E.; Kunert, M.; Menzel, W.; Fortuny-Guasch, J.; Chareau, J.-M.: Human RCS measurements and dummy requirements for the assessment of radar based active pedestrian safety systems, in 14th Int. Radar Symp., Dresden, Germany, 2013, 752–757.

[9] Livingston, E.H.; Lee, S.: Body surface area prediction in normal-weight and obese patients. Am. J. Physiol. Endocrinol. Metab., **281** (2001), E586–E591.

[10] Wisch, M.; Seiniger, P.; Pastor, C.; Edwards, M.; Visvikis, C.; Reeves, C.: Scenarios and weighting factors for pre-crash assessment of integrated pedestrian safety systems, Deliverable 1.1 of the public funded project ASPECSS (EU FP7), chapter 5, 59, 2013, http://www.aspecss-project.eu

[11] Kauppinen, I.; Roth, K.: Audio signal extrapolation – theory and applications, in Proc. of the 5th Int. Conf. on Digital Audio Effects, Hamburg, Germany, 2002, 105–110.

[12] Marple, L.: Resolution of conventional Fourier, autoregressive, and special ARMA methods of spectrum analysis, in IEEE Int. Conf. on Acoustics, Speech, and Signal Processing, 1977, 74–77.

Eugen Schubert was born in Grimma, Germany, in 1986. He received his M.Eng. degree in Information and Communications Engineering from the Hochschule für Telekommunikation, Leipzig, Germany. Currently he is pursuing the Ph.D. degree within the division Chassis Systems Control of the Robert Bosch GmbH, Stuttgart, Germany. His main interests are automotive radar signal processing and pedestrian collision mitigation systems.

Martin Kunert was born in Amorbach, Germany, in 1960. He received his Diploma in Electrical Engineering in 1986 from the University of Munich and received his Ph.D. in digital signal processing from the Institute Nationale Polytechnique of Toulouse, France in 1996. He worked for 22 years in the domain of radar-based driver assistant applications at Siemens VDO and Continental AG and joined the Bosch group in 2008. In the advanced development department within the division Chassis Systems Control he is currently responsible for publicly funded project in the area of driver assistant, safety, and autonomous driving functions.

https://doi.org/10.1017/S1759078715000690 Published online by Cambridge University Press

Frank Meinl received his master degree in Electrical Engineering from the Technische Universität München in 2013. From 2009 to 2011 he was studying at Ecole Centrale Paris in a double-degree program. Since 2013 he is working towards his Ph.D. at the Robert Bosch GmbH within the division Chassis Systems Control. His research topics are focused in the field of algorithms and architectures for radar signal processing as well as rapid prototyping for advanced driver assistance systems.

Wolfgang Menzel received his Dipl.-Ing. degree in Electrical Engineering from the Technical University of Aachen, Germany, in 1974, and his Dr.,-Ing. degree from the University of Duisburg, Germany, in 1977. From 1979 to 1989, he was with the millimeter-wave department at AEG, Ulm, Germany (now EADS). From 1980 to 1985, he was head of the laboratory for Integrated Millimeter-Wave Circuits and from 1985 to 1989 head of the entire millimeter-wave department. During that time, his areas of interest included planar integrated circuits, planar antennas, and systems in the millimeter-wave frequency range. In 1989, he became a Full Professor at the Institute of Microwave Techniques, University of Ulm, Germany. His areas of interest include multilayer planar circuits, waveguide filters and components, antennas, millimeter-wave and microwave interconnects and packaging, millimeter-wave application and system aspects.

https://doi.org/10.1017/S1759078715000690 Published online by Cambridge University Press